

Measurement of the Subcycle Timing of Attosecond XUV Bursts in High-Harmonic Generation

L. C. Dinu and H. G. Muller

FOM Institute for Atomic and Molecular Physics, Kruislaan 407, 1098 SJ Amsterdam, The Netherlands

S. Kazamias, G. Mullot, F. Augé, and Ph. Balcou

Laboratoire d'Optique Appliquée, Ecole Nationale Supérieure des Techniques Avancées (ENSTA) - Ecole Polytechnique CNRS UMR 7639, 91761 Palaiseau Cedex, France

P. M. Paul, M. Kovačev, P. Breger, and P. Agostini

Commissariat à l'Energie Atomique, DSM/DRECAM/SPAM, CE Saclay, 91191 Gif-sur-Yvette, France
(Received 23 January 2003; published 4 August 2003)

The absolute timing of the high-harmonic attosecond pulse train with respect to the generating IR pump cycle has been measured for the first time. The attosecond pulses occur 190 ± 20 as after each pump field maxima (twice per optical cycle), in agreement with the “short” quantum path of the quasiclassical model of harmonic generation.

DOI: 10.1103/PhysRevLett.91.063901

PACS numbers: 42.65.Ky, 42.50.Hz

The process of high-harmonic generation was discovered more than a decade ago [1]. By focusing an infrared (IR) laser (“pump”) beam into a noble-gas jet, high-order odd harmonics of the fundamental radiation are generated. The predicted existence of subfemtosecond (or attosecond) pulses in high-harmonic generation [2–7] was recently demonstrated experimentally [8–10]. Such light pulses open perspectives for “attosecond metrology” [9] and the study of subfemtosecond electron dynamics. If the existence of pulses as short as 250 as was indeed verified, their timing with respect to the generating laser field has never been studied so far.

This Letter demonstrates that this timing can be retrieved experimentally, thus providing an “attosecond clock” that can be used in turn to study the timing of other physical events, e.g., tunnel ionization, with subfemtosecond accuracy.

The timing relies on the measurement of the relative phases of consecutive harmonics by two-color, IR/XUV two-photon ionization. The harmonics and the fundamental beams are focused in a gas jet (the “ionization” region), and the photoelectrons are collected and energy analyzed in a spectrometer. The spectra consist of a series of peaks spaced by twice the IR fundamental photon energy due to photoionization by each harmonic alone and additional peaks, called “sidebands”, exactly in between them (Fig. 1).

Each sideband is due to two interfering, two-photon processes: (i) absorption of one harmonic and one IR photon, and (ii) absorption of one harmonic and emission of one IR photon. The interference gives access to the relative phase between consecutive harmonics and allows a complete reconstruction of the harmonic intensity temporal profile and timing with respect to the probe IR wave at the *ionization* point [8].

In order to recover the timing at the *generation* point, we need to complete this phase retrieval by two more

steps: first the measurement of the absolute timing of the probe/pump fields in the generation region. This is obtained from their interference, detectable in the harmonic generation. Second the evaluation of all phase changes experienced by the harmonics and the probe during the propagation from the generation to the ionization points, due to dispersion, geometrical effects, or other processes.

Analog to [8,11], a Ti:sapphire laser delivers at 1 kHz an IR (800 nm) beam that a mask divides into an outer, annular (“pump”) part and an inner (“probe”) part. The pump is focused into a continuous-flow Ar jet at an intensity of ~ 100 TW/cm². The probe generates the sidebands when combined with the XUV pulses. The delay between pump and probe pulses is adjusted by rotating independently two 6 mm thick glass plates.

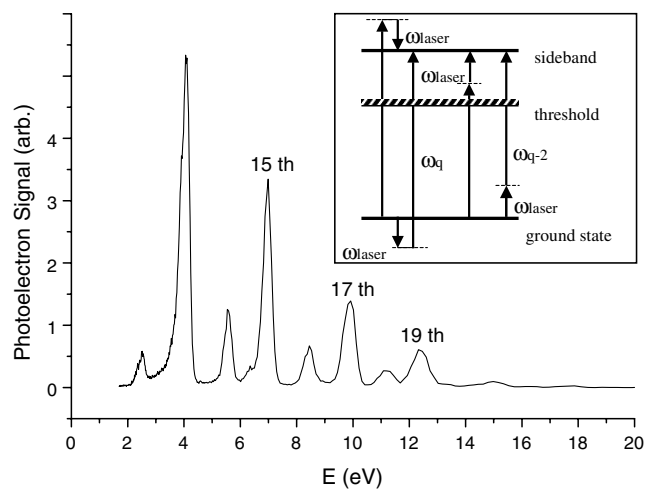


FIG. 1. Photoelectron spectrum of argon exposed to harmonics 11–19 and the IR probe. The single-photon peaks are labeled by the order of the harmonic. The sidebands appear in between. The inset shows the relevant quantum paths.

The annular IR pump is almost entirely blocked by an aperture located after the generation jet. The harmonics, having a divergence much smaller than the pump, and the probe pass unperturbed through that aperture. Both the probe and the XUV are then focused by a Pt-coated toroidal, grazing-incidence mirror into a second Ar jet.

The photoelectrons are collected in a magnetic-bottle time-of-flight spectrometer. Data accumulation uses an analog-to-digital converter at a sampling rate of 250 MHz. Because of space-charge effects and contact potentials we observed only harmonics 13 to 19 but all the sidebands corresponding to orders 12 to 18 are visible in the spectra.

The computer-controlled tilt of the inner delay plate, while keeping the outer plate fixed, determines the delay τ between the probe and the pump pulses. For small angles, τ is given by

$$\tau = A(m - m_0)^2 + B, \quad (1)$$

where A is a constant depending on the angular step of the motor ($0.005^\circ/\text{step}$), the thickness, and the index of refraction of the delay plates. B is a constant depending on the precise tilt of the outer plate and m_0 is the motor position for which the inner plate is exactly perpendicular to the beam.

The total ionization signal S_{tot} is independent of the intensity and phase of the probe which leads only to a redistribution of the photoelectron energies and S_{tot} is just proportional to the amount of generated XUV. Both the pump and the probe pass through the generation focus. Although the probe is about 4 orders of magnitude weaker there, interference is evident in the total signal which is due to the addition of the *fields* and enhanced by the strong nonlinearity of the harmonic-generation process. The intensity of the IR beam, at the focal point, resulting from the superposition of the pump and the probe fields, has the form:

$$I_{\text{gen}} = C + D \cos \omega \tau. \quad (2)$$

From Eqs. (1) and (2), and an order of nonlinearity $N(\approx 9)$:

$$S_{\text{tot}} \sim \{C + D \cos[\omega A(m - m_{\text{cor}})^2 + \omega B]\}^N. \quad (3)$$

Fitting the total signal (Fig. 2) with Eq. (3) determines m_0 and B , and hence the absolute probe-pump delay, as a function of the motor position m .

Hence, the combined action of the harmonics and the probe gives rise to the sidebands, following one of the four quantum paths presented in the inset of Fig. 1. The theory predicts for the amplitude S of a sideband with energy $E_0 + (q - 1)\hbar\omega$ a dependence of the type:

$$S = \sum_f A_f \cos(2\omega_{\text{IR}}\tau + \varphi_{q-2} - \varphi_q + \Delta\varphi_{\text{at}}^f), \quad (4)$$

where A_f and $\Delta\varphi_{\text{at}}^f$ are, respectively, atomic amplitudes

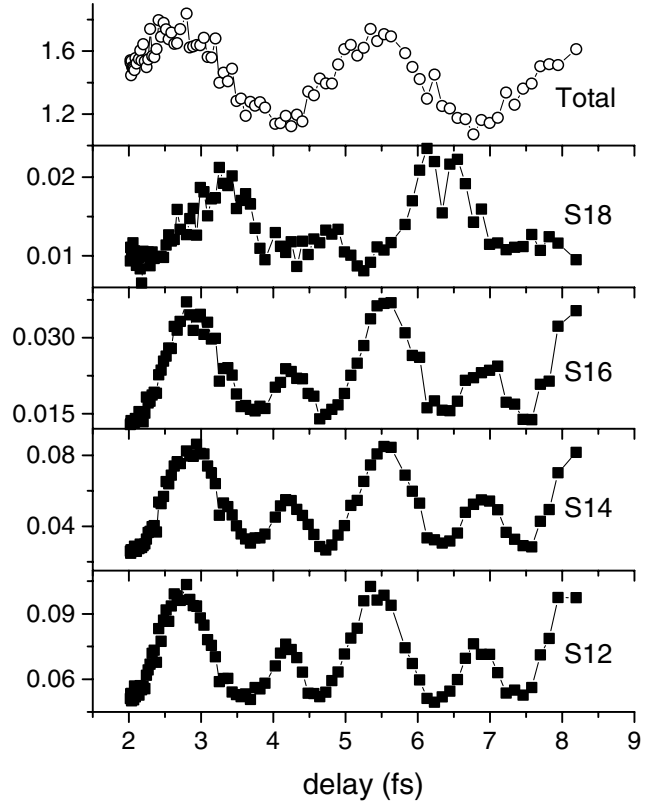


FIG. 2. Energy-integrated ionization signal (top panel) and sideband signals (from $E_0 + 18\hbar\omega$ to $E_0 + 12\hbar\omega$) vs the pump-probe delay. Sideband signals were normalized to the corresponding total signal.

and phases; φ_{q-2} and φ_q are the phases of the harmonics having, respectively, the orders $q - 2$ and q [8]. The amplitudes and phases of all the transitions allowed from the $3p$ state of Ar to the continuum final states denoted by the index f , using linearly polarized light, can be calculated rather accurately [8,12].

Normalizing the data on S_{tot} may be sufficient to remove the dependence on the total XUV flux [8]. However, the present data (Fig. 2) shows a superposition of two oscillations, at frequencies ω_{IR} and $2\omega_{\text{IR}}$, in contradiction with Eq. (4). This can be explained as follows.

Because of the rather high pressure in the generation Ar jet (~ 10 mbar), some IR pump is scattered through the aperture [13] and refocused in the ionization region. Hence, there are actually eight interfering paths, four due to a two-photon ionization harmonics probe and four more due to a harmonics-scattered pump. The sideband signal is then proportional to

$$S = |ae^{i\omega_{\text{IR}}\tau} + be^{-i\omega_{\text{IR}}\tau} + c(ae^{i\varphi_0} + be^{-i\varphi_0})|^2, \quad (5)$$

where a , b are the matrix elements corresponding, respectively, to emission and absorption of one IR photon, φ_0 is a constant phase (of the scattered pump), and c is a

constant representing the ratio of the scattered pump and probe fields.

Beside a dc component, Eq. (5) contains sinusoidal components with frequencies ω_{IR} and $2\omega_{\text{IR}}$. After fitting, the oscillatory component at ω_{IR} and the dc component are subtracted from the sideband signals. This gets completely rid of the effect of the scattered IR pump. Fits based on Eq. (4) of the purified signal for all the sidebands yields the phase differences for the pairs of consecutive harmonics, from the 11th to the 19th. By assigning (arbitrarily) $\varphi_{15} = 0$, the phases of the harmonics are $\varphi_{11} = -1.79$, $\varphi_{13} = -1.08$, $\varphi_{15} = 0$, $\varphi_{17} = 1.09$, and $\varphi_{19} = 2.77$.

The relative amplitudes of the harmonic fields are obtained from the integrated areas of the corresponding peaks for a delay such that the sideband amplitudes are practically negligible, corrected for the known wavelength dependence of the ionization cross sections. For the 11th harmonic, we assumed the same field amplitude as for the 13th harmonic [8]. The resulting amplitudes are in the ratio 11th:13th:15th:17th:19th = 2.76:2.76:1.79:1.26:1.

The total XUV field at the ionization point is

$$E_{\text{XUV}}^{\text{ion}}(t) = \sum_{q=11}^{19} E_q \cos(q\hbar\omega_{\text{IR}}t - \varphi_q). \quad (6)$$

Note that the envelope of the intensity profile of the pulse and its timing with respect to the probe at the ionization point depend only on the harmonics relative phases. If all these phases are shifted by the same amount (i.e., if we would have assigned a nonzero value to φ_{15}), then only the carrier-envelope phase of the pulse is changed.

We now have to evaluate the phase changes between the generation to ionization points. Contributing factors include the Gouy phase slip [14] at focus, the dispersion of the gas medium, and the metallic reflection at the mirror. For harmonics 11 to 19, dispersion contributes 1.66, 1.42, 1.24, 1.07, and 0.98 rad, respectively, assuming that the 0.1 mbar background gas filling the chamber disperses VUV light as one free electron per atom. Those have no observable effect on the shape of the attosecond beats and only displace them in time by about 40 as. The probe phase change, calculated from the atomic dc polarizabilities, is found to be 0.002 rad between the generation and the ionization points. The metallic reflection induces a negligible phase shift for the π -polarized radiation.

As for the Gouy phase, the probe beam, obtained by clipping a small central part of the initial beam, is focused twice, in the generation and ionization points. An accurate beam propagation calculation shows that it incurs a phase change of π between the generation and ionization points. Note that its focusing is very weak, because of its small diameter, and its phase depends very weakly on position: only $7^\circ/\text{cm}$ at the generation point,

and is practically independent of position at the ionization point. The IR pump on the other hand is tightly focused and the optimum point for harmonic generation may be away from the geometrical focus [15], typically by one Rayleigh range, or 1.7 mm in our conditions, so that generation and ionization points might be significantly displaced from the true focus, with corresponding uncertainty in the phase. The harmonics are also focused rather strongly, so their phase slips are substantial. The envelope formed by the beating of several harmonics, however, does not change upon an equal phase change of all the harmonics as already pointed out. This makes the effect of focusing eventually quite negligible for the attosecond beats.

The delayed probe field at the ionization point $E_{\text{probe}}^{\text{ion}}(t, \tau)$ is defined as $\cos[\omega_{\text{IR}}(t - \tau)]$. The delay for which pump and probe phases are equal at the generation point (so their interference there produces a maximum) was defined as $\tau = 0$. Thus at the generation point:

$$E_{\text{pump}}^{\text{gen}} \sim E_{\text{probe(0)}}^{\text{gen}} \sim \cos(\omega_{\text{IR}}t + 0.002). \quad (7)$$

The attosecond pulses, are finally found to occur 190 ± 20 as after each maximum of the driving pump IR electric field (Fig. 3). (The error is derived from the linear fit of the phases versus order). It is interesting to compare this value to the result of the harmonic-generation three-step semiclassical model [16].

In that model, high energy photons are generated when an electron first undergoes tunnel ionization, then is accelerated by the laser field, and eventually recombines radiatively with its parent ion. The kinetic energy gain in the continuum is $\Delta E = 2U_p(\sin(\omega t) - \sin(\omega t'))^2$, where U_p is the ponderomotive potential, t' the ionization time, and t the recombination time (t and t' are easily calculated). The photon energy is then simply $I_p + \Delta E$. For

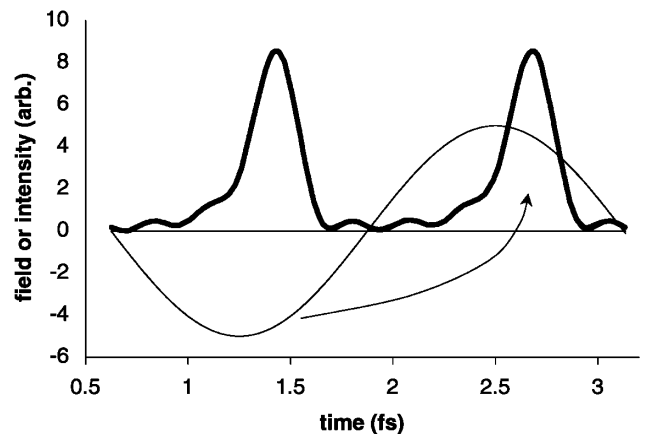


FIG. 3. Intensity envelope of the attosecond beats (thick line) and the IR pump field (thin line). The beat spikes, 266 as FWHM, occur 190 as after the field maxima. A wave packet ejected just after a peak of the field is recolliding with the nucleus (producing the XUV bursts) after about 1520 as.

each harmonic below the cutoff frequency, two paths lead to the same photon energy: electrons ionized very early after the peak of the electric field spend almost one full period in the continuum before recombining (“long” quantum path); electrons ionized slightly later, spend only about half a period in the continuum (“short” quantum path).

For the 15th harmonic (chosen as the middle order of the harmonic comb under consideration) we obtain a short recombination time of 1380 as and a long one of 2320 as. The first result is in excellent agreement with the experimental result ($1333 + 190 = 1523 \pm 150$ as) which excludes the second. This is a new confirmation that the attosecond pulse train arises from the short quantum path in our conditions. The remarkable efficiency of the semi-classical model actually comes as a surprise, as, in argon, ionization does not occur in a pure tunneling regime (Keldysh parameter $\gamma = 1.14$). However, more refined models [17] yield similar timings for the short quantum path and, in a recent numerical study, Gaarde and Schafer [7] have shown that the phase locking is much favored by the short quantum path, again in excellent agreement with our findings.

In conclusion, we have shown that it is possible, by a precise determination of all phase delays between the harmonic-generation point and the detection apparatus, to measure the timing of the attosecond pulses in high-harmonic generation with respect to the pump field cycle. Not only does this yield valuable information on the harmonic-generation process by showing that the short quantum path is dominant, in agreement with the theoretical prediction, but it is the first application of the attosecond pulse train produced by superposing on-phase high harmonics to clocking electron dynamics in strong field interaction.

L. C. D. and H. G. M. participated through the research program of FOM (Fundamenteel Onderzoek der Materie), which is subsidized by NWO (Nederlands Wetenschappelijk Onderzoek), and were also supported by the EC Access Contract No. HPRI-CT-1999-00086.

Support by the ATTO network HPRN-CT-2000-00133 is also acknowledged.

-
- [1] M. Ferray, A. L’Huillier, X. F. Li, L. A. Lompre, G. Mainfray, and C. Manus, *J. Phys. B* **21**, L31 (1988).
 - [2] G. Farkas and C. Toth, *Phys. Lett. A* **168**, 447 (1992).
 - [3] S. E. Harris, J. J. Macklin, and T. W. Hensch, *Opt. Commun.* **100**, 487 (1993).
 - [4] Ph. Antoine, A. L’Huillier, and M. Lewenstein, *Phys. Rev. Lett.* **77**, 1234 (1996).
 - [5] Ph. Antoine, D. B. Milosevic, A. L’Huillier, M. B. Gaarde, P. Salieres, and M. Lewenstein, *Phys. Rev. A* **56**, 4960 (1997).
 - [6] I. P. Christov, M. M. Murnane, and H. C. Kapteyn, *Phys. Rev. A* **57**, R2285 (1998).
 - [7] M. B. Gaarde and K. J. Schafer, *Phys. Rev. Lett.* **89**, 213901 (2002); *Phys. Rev. A* **65**, 031406(R) (2002).
 - [8] P. M. Paul, E. S. Toma, P. Breger, G. Mullot, F. Aug, Ph. Balcou, H. G. Muller, and P. Agostini, *Science* **292**, 1689 (2001).
 - [9] M. Hentschel, R. Kienberger, Ch. Spielmann, G. A. Reider, N. Milosevic, T. Brabec, P. Corkum, U. Heinzmann, M. Drescher, and F. Krausz, *Nature (London)* **414**, 509 (2001).
 - [10] N. A. Papadogiannis, B. Witzel, C. Kalpouzos, and D. Charalambidis, *Phys. Rev. Lett.* **83**, 4289 (1999).
 - [11] E. S. Toma, H. G. Muller, P. M. Paul, P. Breger, M. Cheret, P. Agostini, C. Le Blanc, G. Mullot, and G. Cheriaux, *Phys. Rev. A* **62**, 061801(R) (2000).
 - [12] E. S. Toma and H. G. Muller, *J. Phys. B* **35**, 3435 (2002).
 - [13] Note that this is coherent scattering, namely, the (reproducible) redistribution of pump energy by the gas jet.
 - [14] C. R. Gouy, *Acad. Sci. Paris* **110**, 1251 (1890).
 - [15] A. L’Huillier and Ph. Balcou, *Phys. Rev. Lett.* **70**, 774 (1993).
 - [16] M. Lewenstein, Ph. Balcou, M. Yu. Ivanov, A. L’Huillier, and P. B. Corkum, *Phys. Rev. A* **49**, 2117 (1994).
 - [17] I. P. Christov, M. M. Murnane, and H. C. Kapteyn, *Phys. Rev. Lett.* **78**, 1251 (1997).